Delft University of Technology

Sensitivity of secondary electron yields and SEM images to scattering parameters in MC simulations

Verduin, T.; Lokhorst, S. R.; Hagen, C. W.; Kruit, P.

Important note
To cite this publication, please use the final published version (if applicable).
Please check the document version above.

Sensitivity of secondary electron yields and SEM images to scattering parameters in MC simulations

T. Verduin*, S. R. Lokhorst, C. W. Hagen, P. Kruit

Delft University of Technology
Faculty of Applied Sciences
Department of Imaging Physics
Lorentzweg 1, 2628 CJ Delft, The Netherlands

Abstract

In the simulation of secondary electron yields (SEY) and secondary electron microscopy (SEM) images, there is always the question: "are we using the correct scattering cross-sections?". The three scattering processes of interest are quasi-elastic phonon scattering, elastic Mott scattering and inelastic scattering using the dielectric function model. We have artificially scaled the scattering cross-sections, such that the probability for events associated with a particular model is either increased or decreased. The influence of this adjustment on the calculated SEYs and simulated SEM images is then evaluated. At first we have investigated the influence on the calculated SEY of pure and infinitely thick silicon. We have observed that the influence of the (quasi-elastic) acoustic phonon scattering cross-sections is seen all the way up to the incident primary electron energy of $10\,\text{keV}$. We have extended the analysis to the simulation of SEM images of three dimensional rough lines of PMMA located on a silicon substrate. We conclude that the scaling of the scattering cross-sections affects the contrast of the SEM images, but not the roughness characterization of the lines, i.e. the 3σ of the LER, correlation length and roughness exponent.

Keywords: electron-matter interaction, Monte-Carlo simulation, secondary electron yield, scanning electron microscopy, line edge roughness

*Corresponding author
   Email address:* `T.Verduin@tudelft.nl` (T. Verduin)

1. Introduction

In nano lithography, scanning electron microscopy (SEM) images of resist features are used for dimensional metrology and inspection. The question remains how to interpret the true size, shape and roughness characterization of the three dimensional resist features from two dimensional SEM images. For that purpose, simulation tools can be of great help. Reliable Monte-Carlo electron-matter interaction simulators exist [1, 2], but are unfortunately notoriously slow for SEM image simulation. The performance has been improved by using a triangulated mesh [3] and voxel based geometries [4]. Nevertheless, computation time can still be a problem. A practical example is the determination of line edge roughness (LER) using the power spectral density (PSD), which requires the simulation of multiple images [5]. Recently, we have reduced the computation time further by rewriting the GEANT4 extension from FEI company, see Ref. [1], for the purpose of SEM imaging and lithography simulations [6]. The result is a high-performance simulation tool which includes the refinements for low-energy scattering models from Ref. [1] and acoustic phonon scattering from Ref. [7]. The subject of this article is to investigate the sensitivity of (1) calculated secondary electron yields (SEY) and (2) simulated SEM images of three dimensional patterns of lines and spaces to the parameters of the physical models. The idea is to artificially scale the scattering cross-sections, such that the probability for events associated with a particular model are either increased or decreased. The influence of this adjustment on the calculated SEY and simulated SEM images is then evaluated. By doing so, we can determine the importance of the individual scattering processes with respect to the final result.

2. Model sensitivity analysis

We investigate the cross-section sensitivity by using our own high-performance simulation tool [6] and discriminate between three scattering processes: quasi-

2

elastic phonon scattering [7], elastic Mott scattering [8] and inelastic scattering

using the dielectric function model [9]. The results shown in Figs. 1, 2 and 3 are calculated SEYs of pure and infinitely thick silicon. In each of the three
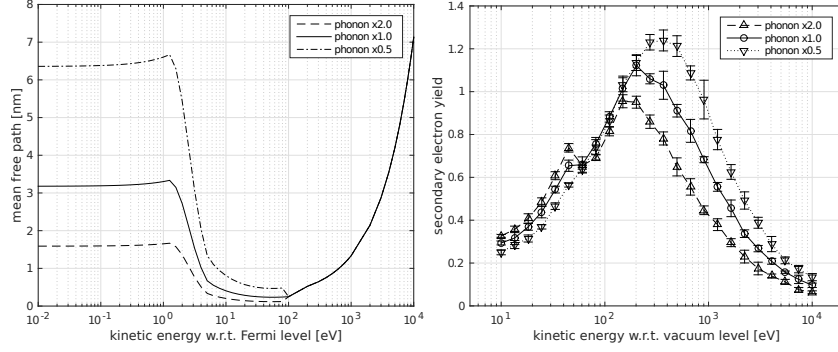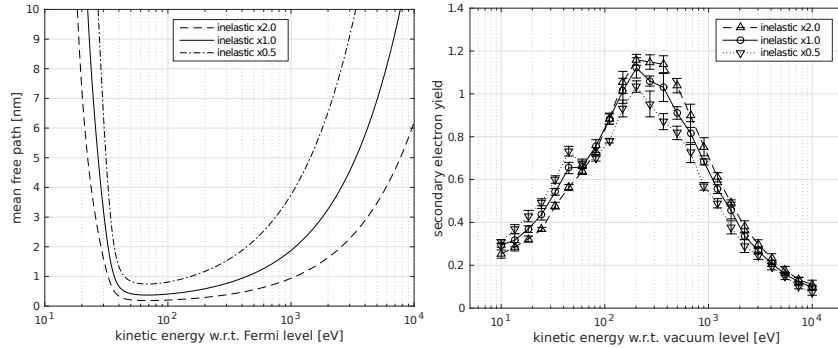

Figure 1: The influence of quasi-elastic phonon scattering cross-sections on the SEY of silicon is shown. In the left image, the scaling of elastic scattering cross-sections, hence the mean free path, is shown. In the right image, the influence of the scaling of elastic scattering cross-sections on the SEY is shown.
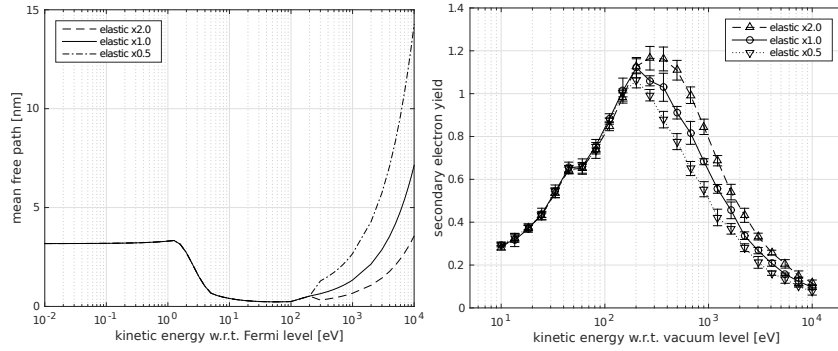
Figure 2: The influence of elastic Mott scattering cross-sections on the SEY of silicon is shown. On the left image, the scaling of elastic scattering cross-sections, hence the mean free path, is shown. On the right image, the influence of the scaling of elastic scattering cross-sections on the SEY is shown.

figures, we have examined the influence of a scattering process by scaling the scattering cross-sections associated with that particular process. Much to our

3

Figure 3: The influence of inelastic cross-sections on the SEY of silicon is shown. On the left image, the scaling of inelastic scattering cross-sections, hence the mean free path, is shown. On the right image, the influence of the scaling of inelastic scattering cross-sections on the SEY is shown.

surprise, we observe that the influence of the (quasi-elastic) acoustic phonon scattering cross-sections in Fig. 1 is seen all the way up to the incident primary electron energy of 10 keV. This is a remarkable effect, because phonon scattering is a low-energy extension to the simulation and is only applied to kinetic energies less than approximately 100 eV. The influence of the acoustic phonon interaction at primary energies higher than 100 eV must stem from the cascading process: electrons with a higher energy ultimately reach, via inelastic scattering events, energy scales at which the coupling to acoustic phonons becomes relevant. In Fig. 2, which corresponds to a scaling of Mott scattering cross-sections, we see no observable effect for electrons with an energy less than 200 eV. In fact, there should be no effect at all[1] because, similarly to the work of Ref. [1], Mott scattering cross-sections are only used for primary energies ranging from 200 eV and upwards. We observe that the sensitivity of the SEY of silicon to the inelastic scattering cross-section in Fig. 3 is comparable to the influence of Mott scattering cross-sections in Fig. 2. Not only the amplitude, but also the kinetic energy at which the maximum SEY occurs, shifts in the same

---

[1]Differences due to statistics are excluded from this statement.

4

direction. By increasing (decreasing) the scattering cross-section, the maximum shifts to the right (left). However, for phonon scattering, in Fig. 1, this is the other way around. Notice that in all three figures a small peak in the SEY is observed near $50\,\text{eV}$. The explanation is found in the way that secondaries are distinguished from backscattered electrons. Below $50\,\text{eV}$ there is no distinction between secondary and backscattered electrons. In other words, *every* emitted electron into the vacuum is simply counted as a secondary electron. From $50\,\text{eV}$ and upwards, we suddenly start to make a distinction between secondary and backscattered electrons based on the kinetic energy. This causes the SEY to slightly decrease because, instead of *all* electrons, a smaller fraction (those with an energy less than $50\,\text{eV}$) are now counted as secondary electrons. By looking at the cross-section sensitivity of the SEY of silicon in Figs. 1, 2 and 3, we conclude that the SEY, for typical beam energies used in CD-SEM metrology and inspection, is most sensitive to the acoustic phonon scattering cross-sections.

We now focus on the sensitivity of simulated SEM images. Our approach is to calculate the SEM image of a fixed pattern of rough lines and spaces for four different cases. The lines are made of PMMA, located on a pure silicon substrate, with dimensions $32\,\text{nm} \times 1\,\mu\text{m} \times 32\,\text{nm}$ (width $\times$ length $\times$ height). The spacing between the lines equals $32\,\text{nm}$. The calculation, in which the pattern is exposed to an electron beam with energy $300\,\text{eV}$, is essentially identical to Ref. [6], except for the fact that for each case, we have scaled the scattering cross-sections of one particular scattering process. In other words, we have obtained one SEM image corresponding to the default scattering cross-sections and three SEM images where either the phonon, elastic Mott or inelastic scattering cross-sections are multiplied by a factor of two. The influence on the resulting SEM images is best seen on the SEM signal profile[2] of a single line, which is shown in Fig. 4. Notice the effect of the PMMA lines on the SEY of the silicon substrate in Fig. 4 (far left and right): the SEY at $300\,\text{eV}$ is higher (approx. 1.5) than in Figs.1, 2 and 3 (approx. 1.1). The primary effect of the scaling of the scattering cross-

---

[2]This profile is obtained by integrating the SEM image of a (rough) line from top to bottom.
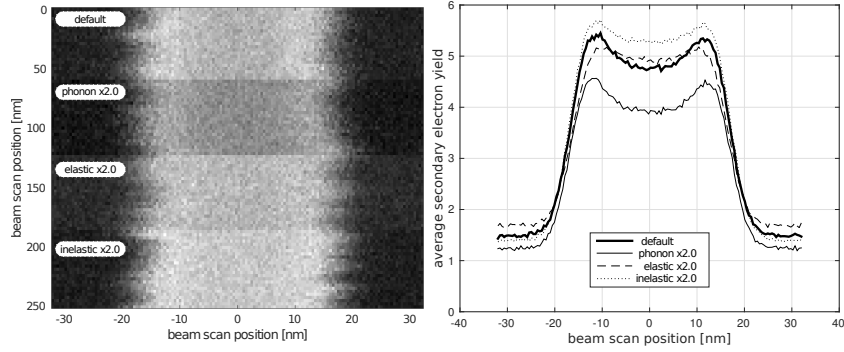
Figure 4: The influence of the scattering cross-sections on a SEM image of rough lines and spaces is shown. On the left image, a composition of the influence of the scattering cross-sections to a small part of the SEM image is shown. The profile (right image) is obtained by integrating the full SEM image (1 µm in length) from top to bottom.

sections is more or less signal in the SEM image. We expect that, in practice, the roughness characterization of the lines remains unaffected. To demonstrate this, we applied the profile based edge-detection method of Ref. [5] to all four SEM images. The result of the roughness characterization (the 3σ LER), including the estimation for the correlation length (ξ) and roughness exponent (α) is given in Table 1 for the four different cases. We conclude that the 3σ of the LER is

scattering cross-sections	3σ [nm]	ξ [nm]	α
default	2.68 ± 0.02	30.3 ± 5.2	0.83 ± 0.09
phonon x2.0	2.72 ± 0.03	34.3 ± 7.4	0.72 ± 0.12
elastic x2.0	2.75 ± 0.02	32.6 ± 5.8	0.80 ± 0.09
inelastic x2.0	2.70 ± 0.02	33.4 ± 7.8	0.75 ± 0.12

Table 1: The roughness characterization of four simulated SEM images of a fixed pattern of rough lines and spaces is shown. Each row corresponds to a separate simulation, where in each simulation only one scattering cross-section is multiplied by a factor of two.

6

indeed not sensitive to the introduced changes in the scattering cross-sections[3]. This demonstrates that the profile based edge-detection, as explained in Ref. [5], is not sensitive to the scaling of the scattering cross-sections.

3. Conclusion

Our sensitivity analysis demonstrates that phonon scattering plays a significant role in the calculation of SEYs. Although phonon scattering has a strong coupling to low energetic electrons, its influence on the SEY of pure silicon is seen all the way up to primary electron energy of $10\,\mathrm{keV}$. We have extended the analysis to the simulation of SEM images of three dimensional rough lines of PMMA located on a silicon substrate. The scaling of the scattering cross-sections affects the contrast of the SEM image, but not the roughness characterization of the lines, i.e. the 3σ of the LER, correlation length and roughness exponent. This means that there is no need to increase the accuracy of the scattering cross-sections. SEM image simulation programs could perhaps be simplified, because the exact cross-sections are not that important.

Acknowledgment

References

[1] Kieft, E. and Bosch, E., "Refinement of Monte Carlo simulations of electronspecimen interaction in low-voltage SEM", *Journal of Physics D: Applied Physics* **41**, 215310 (2008).

---

[3]We have verified that this conclusion also holds when we only multiply the scattering cross-sections of PMMA and leave the scattering cross-sections of silicon untouched.

[2] Villarrubia, J. S., Vladár, A. E., and Postek, M. T., "3D Monte Carlo modeling of the SEM: Are there applications to photomask metrology?", *Proceedings of SPIE* **9236**, 923602 (2014).

[3] Li, Y. G., Mao, S. F., Li, H. M., Xiao, S. M., and Ding, Z. J., "Monte Carlo simulation study of scanning electron microscopy images of rough surfaces", *Journal of Applied Physics* **104** (2008).

[4] Lawson, R. A. and Henderson, C. L., "Understanding the relationship between true and measured resist feature critical dimension and line edge roughness using a detailed scanning electron microscopy simulator", *Journal of Vacuum Science & Technology B: Microelectronics and Nanometer Structures* **28**, C6H34 (2010).

[5] Verduin, T., Kruit, P., and Hagen, C. W., "Determination of line edge roughness in low dose top-down scanning electron microscopy images", *Journal of Micro/Nanolithography, MEMS, and MOEMS* **13**, 033009 (2014).

[6] Verduin, T., Lokhorst, S. R., Kruit, P., and Hagen, C. W., "The effect of sidewall roughness on line edge roughness in top-down scanning electron microscopy images", *Proceedings of SPIE*, **9424**, 942405 (2015).

[7] Schreiber, E. and Fitting, H. J., "Monte Carlo simulation of secondary electron emission from the insulator SiO2", *Journal of Electron Spectroscopy and Related Phenomena* **124**, 25–37 (2002).

[8] Salvat, F., Jablonski, A., and Powell, C. J., "ELSEPA – Dirac partial-wave calculation of elastic scattering of electrons and positrons by atoms, positive ions and molecules", *Computer Physics Communications* **165**, 157–190 (2005).

[9] Ashley, J., "Interaction of low-energy electrons with condensed matter: stopping powers and inelastic mean free paths from optical data", *Journal of Electron Spectroscopy and Related Phenomena* **46**, 199–214 (1988).